Three-Coordinate Rhodium Complexes in Low Oxidation States

Varela-Izquierdo, V.; López, J.A.; de Bruin, B.; Tejel, C.; Ciriano, M.A.

DOI
10.1002/chem.202000387
Publication date
2020
Document Version
Final published version
Published in
Chemistry-A European Journal

ChemPubSoc Europe

DOI: 10.1002/chem.202000387

CHEMISTRY A European Journal Communication

Electron-Deficient Compounds

Three-Coordinate Rhodium Complexes in Low Oxidation States

Víctor Varela-Izquierdo,[a] José A. López,[a] Bas de Bruin,[b] Cristina Tejel,*[a] and Miguel A. Ciriano*[a]

Abstract: The isolation of simultaneously low-coordinate and low-valent compounds is a timeless challenge for preparative chemists. This work showcases the preparation and full characterization of tri-coordinate rhodium(-I) and rhodium(0) complexes as well as a rare rhodium(I) complex. Reduction of $[\{Rh(\mu\text{-}Cl)(IPr)(dvtms)\}_2]$ (**1**, IPr = 1,3-bis(2,6-diisopropylphenyl)imidazolyl-2-ylidene; dvtms = divinyltetramethyldisiloxane) with KC_8 gave the trigonal complexes K[Rh(IPr)(dvtms)] and [Rh(IPr)(dvtms)], whereas the cation $[Rh(IPr)(dvtms)]^+$ results from their oxidation or by abstraction of chloride from **1** with silver salts. The paramagnetic Rh^0 complex is a unique fully metal-centered radical with the unpaired electron in the d_{z2} orbital. The Rh(-I) complex reacts with PPh_3 with replacement of the NHC ligand, and behaves as a nucleophile, which upon reaction with $[AuCl(PPh_3)]$ generates the trigonal pyramidal complex [(IPr)(dvtms)Rh-Au(PPh_3)] with a metal–metal bond between two d^{10} metal centers.

Low-valent transition-metal complexes that simultaneously have low coordination numbers are highly reactive species, which have been proposed as intermediates in transition-metal catalyzed reactions.[1] This class of compounds can mediate chemical bond activations and are a source of unusual compounds with new electronic properties. From a synthetic point of view, the stabilization of metal atoms in low oxidation states and with low coordination numbers has been a challenging target for decades. Typically, carbon monoxide, olefins, and phosphines have been utilized to stabilize low-valent metal compounds. Despite their much higher σ-donation properties (NHC→M), NHC ligands have favorably replaced phosphine ligands for this purpose, taking advantage of their bulkiness.[2] Thus, zero-valent low-coordinate palladium and platinum complexes with NHCs are well-known compounds[3] and there are quite a few complexes of the first-row transition metals of this type.[4] However, to date low oxidation state rhodium(0) or rhodium(-I) compounds with NHC ligands have remained unreported.

Rh^0 and Rh(-I) compounds have been known for 50 years. Many of them were electrochemically generated as short-lived intermediates,[5] or isolated as complexes with strong π-acceptor ligands such as $[Rh(CO)_4]^-$ or $[Rh(PF_3)_4]^-$, and as polynuclear clusters.[6] Afterwards, fully characterized d^9-ML_4 and d^{10}-ML_4 compounds with diphosphines,[7] and mixed olefin-phosphine ligands have been reported and extensively studied by Grützmacher (Scheme 1).[8] They are typically tetracoordinate, thus

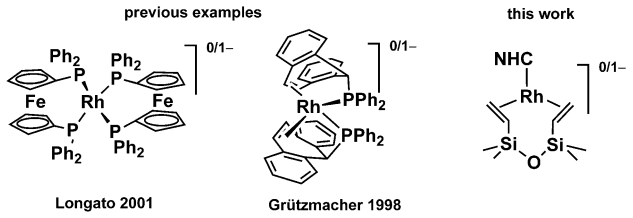

Scheme 1. Previously known d^9- and d^{10}-ML_4 compounds and the d^9-, and d^{10}-ML_3 complexes presented in this work.

following the 18-electron rule, and display more or less distorted tetrahedral structures, except the distinctive trigonal pyramidal $[K(thf)_3][P_3^{Si}Rh]$ [P_3^{Si} = tris(*o*-diisopropylphosphinophenyl)-silylide.[9] Those of Rh^0 have been characterized and many of them fully studied by EPR spectroscopy and DFT methods.[10] Interestingly, they are all highly delocalized radicals, with the exception of one metal-centered radical, [Rh($trop_2PPh$)(PPh_3)], [ρ(Rh) 58%], which is in electromeric equilibrium with the delocalized radical.[11] In any case, isolated compounds of rhodium in the oxidation states 0 and −1 are rare and their chemistry is underdeveloped.

Regarding this general panorama, we decided to explore reduction reactions of NHC rhodium complexes to confirm if electron-rich metal centers are compatible with strong σ-donor ligands in the coordination sphere of rhodium. Herein, we describe the preparation and properties of the first isolated NHC rhodium(0) and rhodium(-I) complexes, which are unique examples of low-valent and low-coordinate rhodium complexes in a trigonal planar environment, and some of their reactions.

The election of the ancillary ligands is crucial for stabilizing the products. For example, reduction of [RhCl(IPr)(cod)] (IPr =

[a] V. Varela-Izquierdo, Dr. J. A. López, Dr. C. Tejel, Prof. Dr. M. A. Ciriano
Departamento de Química Inorgánica
Instituto de Síntesis Química y Catálisis Homogénea (ISQCH), CSIC
Universidad de Zaragoza
Pedro Cerbuna 12, 50009 Zaragoza (Spain)
E-mail: ctejel@unizar.es
mciriano@unizar.es

[b] Prof. Dr. B. de Bruin
Van't Hoff Institute for Molecular Sciences
University of Amsterdam
Science Park 904, 1098 XH Amsterdam (The Netherlands)

Supporting information and the ORCID identification number(s) for the author(s) of this article can be found under:
https://doi.org/10.1002/chem.202000387.

1,3-bis(2,6-diisopropylphenyl)imidazolyl-2-ylidene; cod = 1,5-cyclooctadiene) with KC_8 in thf does occur, but the intermediate species undergoes further transformations that will be reported elsewhere. We only succeed in isolation of the primary reduced species when using an open and more adaptable chelating diolefin than cod, such as divinyltetramethyldisiloxane (dvtms). The precursor complex [{Rh(μ-Cl)(IPr)(dvtms)}$_2$] (**1**) was prepared and characterized by X-ray and conventional methods. Complex **1** is dinuclear with two chloride bridges, the diolefin coordinated by only one vinyl η^2-C=C bond, and the NHC ligands in a *transoid* disposition. The complex is fluxional in solution, but the low-temperature NMR spectra are consistent with the structure found in the solid state. For comparative purposes, the NMR chemical shifts and C=C bond distances of the coordinated and non-coordinated ligand double bonds are presented in Table S1 (Supporting Information).

Reduction of **1** with KC_8 in thf takes place in two steps to give first [Rh(IPr)(dvtms)] (**2**), and then K[Rh(IPr)(dvtms)] K[**2**] (Scheme 2). Additionally, comproportionation of K[**2**] with **1** in thf occurs to give **2** immediately, providing thus a second method to isolate **2** cleanly. A similar comproportionation reaction to **2** was observed by reacting K[Rh(IPr)(dvtms)] (K[**2**]) with [Rh(IPr)(dvtms)]PF_6 ([**2**]PF_6) (see below).

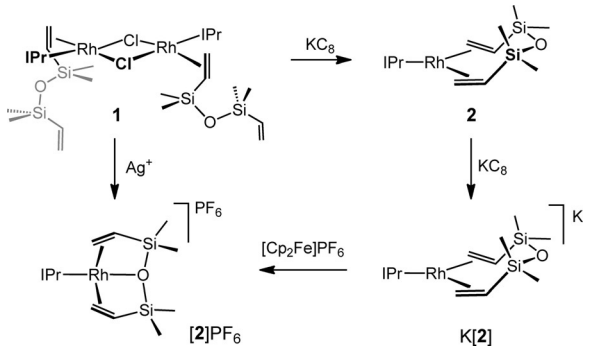

Scheme 2. Reactions giving tri-coordinate Rh(-I), Rh^0 and square-planar Rh^I complexes.

Complexes **2** and K[**2**] were isolated as very sensitive to oxygen and moisture crystalline brown-orange solids after workup. Their X-ray structures (Figure 1) revealed they are trigonal-planar complexes with the metals bound to the NHC ligand and to dvtms through both C=C bonds with all the carbon atoms virtually in the molecular plane.

This feature contrasts with the C=C bond coordination perpendicular to the molecular plane of olefins in square-planar Rh^I complexes. The "planar" disposition leads to strong π-back donation, as revealed by the long C=C bond distances of ca. 1.43 Å in **2** and K[**2**] compared with that of the free bond in **1** (1.30 Å). Hence, the Rh^0 and (Rh(-I) diene complexes **2** and K[**2**] can also be described by their corresponding Rh^{II} and Rh^I metalacyclopropane resonant structures, respectively.

The diamagnetic complex K[**2**] maintains in solution the structure found in the solid state, although a more symmetric averaged molecule is observed by NMR spectroscopy due to

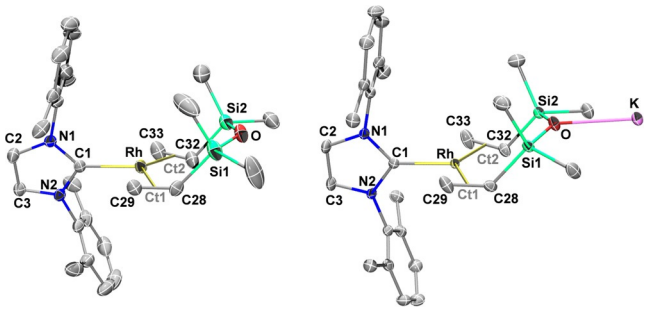

Figure 1. Molecular structure (ORTEP, ellipsoids set at 50% probability) of complexes [Rh(IPr)(dvtms)] (**2**) (left) and K[Rh(IPr)(dvtms)] K[**2**] (right). Selected bond distances [Å] and angles [°] for **2**: Rh–C1 2.092(3), Rh–Ct1 2.024(4), Rh–Ct2 2.030(4), C28–C29 1.422(6), C32–C33 1.421(6), C1-Rh-Ct1 111.2(2), C1-Rh-Ct2 117.3 (2), Ct1-Rh-Ct2 130.6(2); for K[**2**]: Rh–C1 2.0363(13), Rh–Ct1 1.990(4), Rh–Ct2 1.989(1), C28–C29 1.435(2), C32–C33 1.436(2), C1-Rh-Ct1 112.3(1), C1-Rh-Ct2 111.7(1), Ct1-Rh-Ct2 135.9(1). Ct1 and Ct2 are middle points of C28,29 and C32,C33, respectively. Only CH carbons of the *i*Pr groups are shown for clarity.

the free rotation of the phenyl groups and the imidazolyl-2-ylidene ring around the C–N and C–Rh bonds, respectively. The shift to high field of the vinyl protons and carbons that appear in the aliphatic region is noticeable and in agreement with strong π-back donation (Table S1, Supporting Information). In addition, the carbene carbon is observed at low field and shifted up to ca. 60 ppm relative to complex **1**.

The Rh^0 complex **2** is paramagnetic. The magnetic moment (1.7 μB, Evans' method) is in agreement with an $S = {}^1/_2$ ground state with one unpaired electron. It shows broad signals in the ^{1}H NMR spectrum, in the range between $\delta = -10$ and 110 ppm. The EPR spectrum of **2** (Figure 2, left) reveals a rhombic (nearly axial) *g*-tensor with large *g*-anisotropy. A satisfactory simulation was obtained using the parameters shown in Table 1. The large deviations of the *g*-values from g_e and the relatively large Rh hyperfine couplings (well-resolved along g_{11}) show that the unpaired electron of complex **2** resides in a mainly metal-centered SOMO. This was confirmed by supporting DFT calculations, showing that the unpaired electron of **2** resides predominantly in the metal d_{z2} orbital (Figure 2, right).

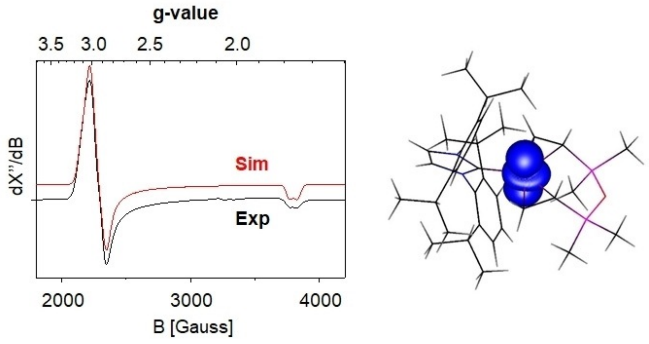

Figure 2. Experimental and simulated EPR spectrum of **2**. Experimental parameters: Microwave frequency = 9.392888 GHz, microwave power = 0.632 mW, mod. amplitude = 2 Gauss, temp. = 10 K (left) and spin density plot of **2** showing that the unpaired electron resides almost entirely in the Rh d_{z2} orbital (right).

Table 1. Experimental and DFT calculated EPR parameters of **2**.

	Exp. (spectral simulation)	DFT[a]
g_{11}	1.766	1.932
g_{22}	2.920	2.818
g_{33}	3.060	2.900
A^{Rh}_{11} [b]	150 MHz	−183 MHz
A^{Rh}_{22} [b]	NR (200 MHz)[c]	−229 MHz
A^{Rh}_{33} [b]	NR (220 MHz)[c]	−247 MHz

[a] ADF, B3LYP, TZ2P, collinear unrestricted spinorbit ZORA. [b] Rhodium hyperfine interaction tensor. [c] NR = not resolved. Values between brackets are rough estimated values based on line shape analysis, assuming that the experimental line width is smaller than the Rh hyperfine interactions.

The DFT calculated EPR parameters of **2** are in good agreement with the experimental parameters (Table 1). In contrast to all the previously reported formal rhodium(0) complexes,[9,10,11] complex **2** is a genuine metal-centered radical.

Cyclic voltammetry measurements on the radical-complex **2** in thf revealed a redox couple centered at −1.36 V (versus SCE) corresponding to the **2**⇄[**2**]$^-$ process. The shape of this wave indicates a further irreversible chemical reaction undergone by the electrogenerated anion [**2**]$^-$ because values of i_{pa}/i_{pc} were <1, and they increased as the scan rate does, reaching a value of 0.6 at a 500 mV s^{-1}. This lack of reversibility could be attributed to the adventitious presence of traces of oxygen or water that destroy the anionic complex [**2**]$^-$. A second wave, fully irreversible in this case, was observed at −0.1 V, which has been assigned to the one-electron oxidation reaction of **2** to the cationic complex [**2**]$^+$. The irreversibility observed in this case is due to a change in the coordination environment of rhodium (see below).

The low potential at which complex **2** is oxidized makes feasible its chemical oxidation (also expected for [**2**]$^-$) by $[Cp_2Fe]PF_6$. Accordingly, oxidation of K[**2**] with $[Cp_2Fe]PF_6$ in thf (1:2 molar ratio) provides the orange cationic complex [Rh(IPr)(dvtms)]PF_6 ([**2**]PF_6), which was isolated as a microcrystalline solid in good yield. This compound can be also prepared by abstraction of chloride from **2** with thallium or silver salts. Complex [**2**]PF_6 should be isolated quickly since it decomposes slowly in thf and undergoes a fast replacement of the olefin dvtms in acetonitrile to give $[Rh(IPr)(MeCN)_3]PF_6$.[12] All attempts to grow monocrystals of [**2**]PF_6 failed, but we succeeded by replacing the counteranion PF_6^- by BF_4^-. The structure of the cation in [**2**]BF_4 is shown in Figure 3.

The rhodium atom in [**2**]$^+$ shows a distorted square-planar environment bound to the carbon (C1) of the carbene and to a highly tensioned divinyltetramethyldisiloxane (dvtms) through both C=C bonds and the oxygen atom as a rare tridentate pincer ligand. Oxygen displays a highly distorted geometry, close to a T-shaped arrangement with a Si1-O-Si2 angle of 160.4(2)°, as can be clearly observed in Figure 3. Both C=C bonds are placed in between the "planar" orientation found in **2** and [**2**]$^-$ and the typical orthogonal disposition for rhodium(I) complexes. The C=C bond distances of 1.370(6) and 1.378(6) Å are quite shorter than in complexes **2** and [**2**]$^-$, in agreement with a smaller extension of the π-back donation expected for a Rh^I center. The cation [**2**]$^+$ was found to be fluxional a r.t., but the ^{1}H and ^{13}C{^{1}H} NMR spectra at −50 °C ($CDCl_3$) agreed with a species having a C_2 symmetry axis that makes the two halves of the molecule equivalent. On raising the temperature, broad-line effects on the resonances corresponding to the aryl groups were observed. Noticeably, one can also observe the coalescence and emergence as a singlet of the methyl groups bonded to silicon, which requires the formal inversion of the oxygen atom. From the VT-^{1}H NMR spectra, the activation parameters for this process were found to be $\Delta H^{\neq} = 20.0 \pm 0.7$ kcal mol^{-1} and $\Delta S^{\neq} = 18.2 \pm 1.1$ cal mol^{-1} K^{-1} ($\Delta G^{\neq}_{298} = 14.6$ kcal mol^{-1}). The positive value for $\Delta S^{\neq}$ evidences a more disordered transition state that has to be related with the cleavage of the Rh–O bond. A further inversion of the six-membered metallacycle (Rh-Ct1-Si1-O-Si2-Ct2) followed by coordination of oxygen accounts for the observed dynamics. Indeed, the Rh–O bond is weak and can be easily broken down. Accordingly, the O-bound species [Rh(IPr)(dvtms)] ([**2**]$^+$) was computed to be only 9.8 kcal mol^{-1} more stable than that with the dissociated O-atom.

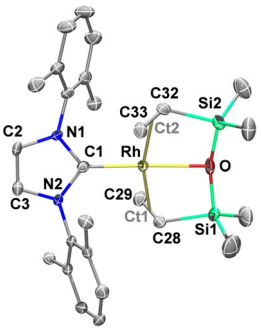

Figure 3. Molecular structure (ORTEP, ellipsoids set at 50% probability) of the cation [Rh(IPr)(dvtms)] ([**2**]$^+$). Selected bond lengths [Å] and angles [°] for [**2**]$^+$: Rh–C1 1.972(4), Rh–O 2.212(3), Rh–Ct1 2.087(4), Rh–Ct2 2.102(4), C28–C29 1.370(6), C32–C33 1.378(6), C1-Rh-O 178.01(13), Ct1-Rh-Ct2 165.6(2). Ct1 and Ct2 are middle points of C28,29 and C32,C33, respectively. Only CH carbons of the *i*Pr groups are shown for clarity.

The Rh(-I) complex K[**2**] reacts with triphenylphosphine, which replaces the IPr ligand to give K[Rh(PPh_3)(dvtms)] (K[**3**]), a reaction opposite to the early syntheses of NHC complexes in which phosphine was changed by NHC ligands (Figure 4).[3a] Most probably the difference in the π-accepting properties of both ligands is the driving force of the reaction. The geometry

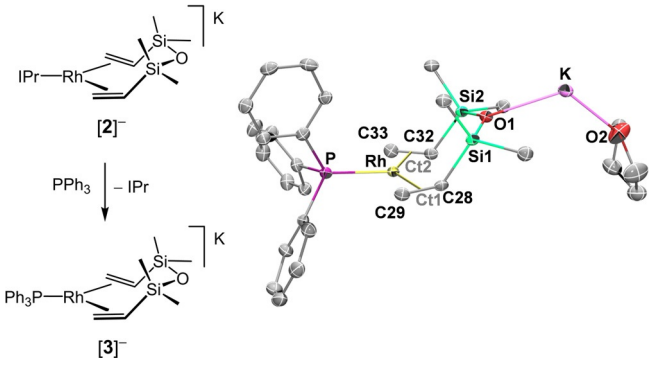

Figure 4. Replacement of IPr by PPh_3 to give a new tricoordinate Rh(-I) complex and molecular structure (ORTEP, ellipsoids set at 50% probability) of K[Rh(PPh_3)(dvtms)]·thf. Selected bond lengths [Å] and angles [°]: Rh–P 2.2371(11), Rh–Ct1 2.008(4), Rh–Ct2 2.008(4), C28–C29 1.429(6), C32–C33 1.433(6), P-Rh-Ct1 110.66(12), P-Rh-Ct2 114.20(12), Ct1-Rh-Ct2 135.1(2). Ct1 and Ct2 are middle points of C28,29 and C32,C33, respectively.

around rhodium is again trigonal-planar, bound to the phosphorus atom and to both C=C bonds, again in a "planar" orientation. The C=C bond lengths were found to be similar to those in K[**2**], although their NMR data exhibited a low-field shift of the signals relative to K[**2**] in the ^{1}H and ^{13}C NMR spectra. These shifts agree with a smaller extension of the π-back donation from Rh to the C=C bonds because of the better π-accepting properties of PPh_3 than IPr, which on the whole stabilizes complex K[**3**].

Reaction of the anionic complex K[**2**] with [AuCl(PPh_3)] gave the neutral complex [(IPr)(dvtms)RhAu(PPh_3)] (**4**) that features a metal–metal bond and a trigonal pyramidal structure with the gold atom at the apex (Figure 5).

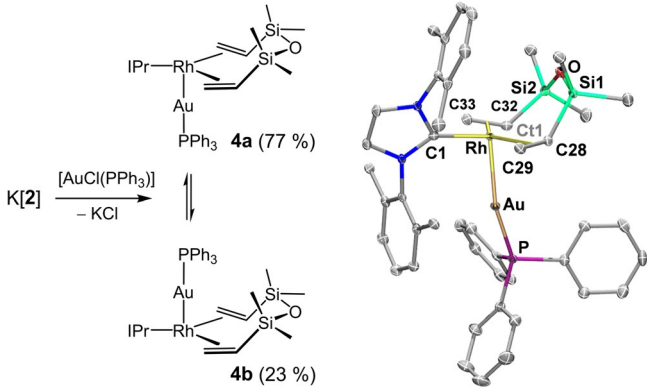

Figure 5. Synthesis of complex [(IPr)(dvtms)RhAu(PPh_3)] (**4**) and molecular structure (ORTEP, ellipsoids set at 50% probability) of the major isomer **4a**. Selected bond distances [Å] and angles [°]: Rh–Au 2.5302(3), Rh–C1 2.073(2), Rh–Ct1 2.018(2), Rh–Ct2 2.021(2), C28–C29 1.434(3), C32–C33 1.431(3), Au–P 2.2477(7), C1-Rh-Ct1 114.96(9), C1-Rh-Ct2 109.79(9), Ct1-Rh-Ct2 134.86(10), Rh-Au-P 163.13(2). Ct1 and Ct2 are middle points of C28,29 and C32,C33, respectively. Only CH carbons of the *i*Pr groups are shown by clarity.

Complex **4** exists in solution as a mixture of two interconverting isomers **4a**/**4b** from which the most abundant **4a** (77%) is the only one found in the solid state. The main difference between these structures is the position of the Au(PPh3) fragment relative to the basal plane, as deduced by NMR methods (see Supporting Information). The topology of the basal plane is similar to that of complexes **2**, [**2**]$^{-}$, and [**3**]$^{-}$, including the C=C bond distances. Whereas the chemical shifts of the olefinic protons in **4a**/**4b** are low-field shifted relative to those of [**2**]$^{-}$, the olefin ^{13}C chemical shifts are similar to those of [**3**]$^{-}$, which is indicative of a smaller back-donation to the olefin than in [**2**]$^{-}$.

Complex **4** can be considered as either a covalent Rh^0–Au^0 complex or Rh(-I)–Au^{I} complex with a dative metal–metal bond. We favor the latter description, based on the structure and the above NMR data. Moreover, NBO-analysis showed charges on the metals to be 0.28307 (Au) 0.07809 (Rh) and a Wiberg bond index 0.60973. As such, complex **4** represents a rare complex with two interacting closed-shell d^{10} centers.

Both isomers **4a**/**4b** decompose in [D_8]toluene slowly and cleanly up to the half-life = 13.5 h through an exchange of the IPr and PPh_3 ligands on gold and rhodium (Scheme 3). The

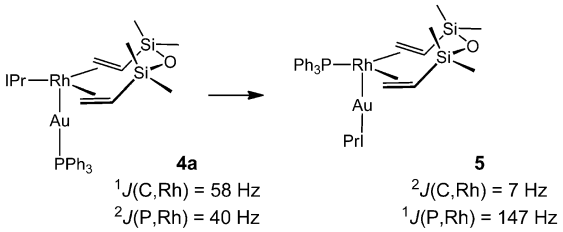

Scheme 3. Transformation of **4a** in complex **5**.

new complex **5** was characterized by NMR methods, which clearly indicated the coordination of the NHC to gold and the phosphine to rhodium (see Supporting Information). In particular, key data were the changes in the coupling constants *J*(C,Rh) and *J*(P,Rh) on going from **4a** to **5** (see Scheme 3). Also relevant is the shift to high field of the N-C-N carbon bonded to gold (δ = 208.4 ppm in **4a**, and 166.2 ppm in **5**).

DFT studies on complexes **4a** and **5** indicated that **5** is 14.4 kcal mol^{-1} more stable than **4a**, which can be attributed to a smaller steric clash between the PPh_3 and NHC ligands in **5**. Moreover, the Rh–Au bond length was found to be slightly shorter in **5** (2.525 Å) than in **4a** (2.547 Å), whereas the Wiberg bond indexes indicate a stronger Rh–Au bond in **5** (0.88811) than in **4a** (0.60973). Moreover, according to the natural charges on the metals (Au, 0.34900; Rh, −0.07240) complex **5** contains a more polarized metal–metal bond.

In conclusion, we showcase the synthesis of novel and unique tri-coordinate rhodium(0) and rhodium(-I) complexes. Thus, K[Rh(IPr)(dvtms)] was isolated from the reduction of [{Rh(μ-Cl)(IPr)(dvtms)}$_2$] with KC_8, while the triphenylphosphine analogue arises from the easy ligand replacement of IPr by PPh_3. One-electron reduction of the Rh^{I} complex gave the rhodium(0) complex [Rh(IPr)(dvtms)], a unique 15 VE. localized metal-centered radical. Moreover, the anionic Rh(-I) complex reacts with [AuClPPh_3] to give the trigonal pyramidal complex [(IPr)(dvtms)Rh-Au(PPh_3)], with a metal–metal bond between two d^{10} metal centers. Further studies on these very reactive complexes are currently in progress.

Acknowledgements

The generous financial support from MINECO/FEDER/AGE (CTQ2017-83421-P, C.T.), Gobierno de Aragón/FEDER (GA/FEDER, Inorganic Molecular Architecture Group E08_17R; C.T.) and the Netherlands Organization for Scientific Research (NWO) (TOP Grant 716.015.001, BdB) is gratefully acknowledged. V.V.-I. thanks MINECO/FEDER for a FPI fellowship.

Conflict of interest

The authors declare no conflict of interest.

Keywords: low-valent · metal–metal bond · NHC ligands · rhodium · tri-coordinate

[1] a) P. P. Power, *Chem. Rev.* **2012**, *112*, 3482 – 3507; b) S. Roy, K. C. Mondal, H. W. Roesky, *Acc. Chem. Res.* **2016**, *49*, 357 – 369; c) L. J. Taylor, D. L. Kays, *Dalton Trans.* **2019**, *48*, 12365 – 12381.

[2] a) M. N. Hopkinson, C. Richter, M. Schedler, F. Glorius, *Nature* **2014**, *510*, 485 – 496; b) H. V. Huynh, *Chem. Rev.* **2018**, *118*, 9457 – 9492.

[3] a) I. E. Markó, S. Stérin, O. Buisine, G. Mignani, P. Branlard, B. Tinant, J. P. Declercq, *Science* **2002**, *298*, 204 – 206; b) S. Fantasia, H. Clavier, S. P. Nolan in *Encyclopedia of Inorganic Chemistry* (eds.: R. B. King, R. H. Crabtree, C. M. Lukehart, D. A. Atwood, R. A. Scott), Wiley, New York, **2008**, https://doi.org/10.1002/0470862106.ia460; c) F. Hering, J. Nitsch, U. Paul, A. Steffen, F. M. Bickelhaupt, U. Radius, *Chem. Sci.* **2015**, *6*, 1426.

[4] a) A. A. Danopoulos, T. Simler, P. Braunstein, *Chem. Rev.* **2019**, *119*, 3730 – 3961; b) J. Cheng, Q. Chen, X. Leng, Z. Ouyang, Z. Wang, S. Ye, L. Deng, *Chem* **2018**, *4*, 2844 – 2860 and references therein.

[5] J. Orsini, W. E. Geiger, *J. Electroanal. Chem.* **1995**, *380*, 83 – 90.

[6] a) F. H. Jardine in *Comprehensive Coordination Chemistry, Vol 4*, (Eds.: G. Wilkinson, R. D. Gillard, J. A. McCleverty), Pergamon Press, Oxford, **1987**, p. 901; b) R. P. Hughes in *Comprehensive Organometallic Chemistry Vol. 5* (Eds.: E. W. Abel, F. G. A. Stone, G. Wilkinson), Pergamon Press, Oxford, **1982**, p. 277; c) P. R. Sharp in *Comprehensive Organometallic Chemistry II, Vol. 8* (Eds.: E. W. Abel, F. G. A. Stone, G. Wilkinson), Pergamon Press, Oxford, **1995**, p. 115.

[7] B. Longato, R. Coppo, G. Pilloni, C. Corvaja, A. Toffoletti, G. Bandoli, *J. Organomet. Chem.* **2001**, *637 – 639*, 710 – 718.

[8] H. Schönberg, S. Boulmaâz, M. Wörle, L. Liesum, A. Schweiger, H. Grützmacher, *Angew. Chem. Int. Ed.* **1998**, *37*, 1423 – 1426; *Angew. Chem.* **1998**, *110*, 1492 – 1494.

[9] P. J. Nance, N. B. Thompson, P. H. Oyala, J. C. Peters, *Angew. Chem. Int. Ed.* **2019**, *58*, 6220 – 6224; *Angew. Chem.* **2019**, *131*, 6286 – 6290.

[10] B. de Bruin, J. C. Russcher, H. Grützmacher, *J. Organomet. Chem.* **2007**, *692*, 3167 – 3173.

[11] F. F. Puschmann, J. Harmer, D. Stein, H. Rüegger, B. de Bruin, H. Grützmacher, *Angew. Chem. Int. Ed.* **2010**, *49*, 385 – 389; *Angew. Chem.* **2010**, *122*, 395 – 399.

[12] L. Palacios, A. Di Giuseppe, A. Opalinska, R. Castarlenas, J. J. Pérez-Torrente, F. J. Lahoz, L. A. Oro, *Organometallics* **2013**, *32*, 2768 – 2774.

Manuscript received: January 22, 2020

Accepted manuscript online: January 27, 2020

Version of record online: February 19, 2020

